

INACTIVE

JUN 10 1948 REC'D

CLASSIFICATION CANCELLED

Copy No. /
RM No. SL8E28a

*McDonnell
P 88/2*

~~Confidential File~~
PERMANENT FILE COPY

NACA

RESEARCH MEMORANDUM

for the

Air Materiel Command, U. S. Air Force

PRELIMINARY RESULTS OF AN INVESTIGATION BY THE WING-FLOW METHOD
OF THE LONGITUDINAL STABILITY CHARACTERISTICS OF A $\frac{1}{50}$ -SCALE
SEMISPAN MODEL OF THE MCDONNELL XP-88 AIRPLANE

By

Harold L. Crane

Langley Memorial Aeronautical Laboratory
Langley Field, Va.

CLASSIFICATION CANCELLED

This document contains classified information affecting the National Defense of the United States within the meaning of the Espionage Act, USC 5031 and 5041. Its transmission or the revelation of its contents in any manner to an unauthorized person is prohibited by law. Information so classified may be imparted only to persons in the military and naval services of the United States, appropriate civilian officers and employees of the Federal Government who have a legitimate interest therein, and to United States citizens of known loyalty and discretion who of necessity must be informed thereof.

7-20-55

NACA change # 3025

Status: INACTIVE

**NATIONAL ADVISORY COMMITTEE
FOR AERONAUTICS FILE COPY**

WASHINGTON

JUN 9 1948

To be returned to
the files of the
Adv. Com. nittee

To Aeronautics
Washington, D. C.

CLASSIFICATION CANCELLED

5287875

19



NATIONAL ADVISORY COMMITTEE FOR AERONAUTICS

RESEARCH MEMORANDUM

for the

Air Materiel Command, U. S. Air Force

PRELIMINARY RESULTS OF AN INVESTIGATION BY THE WING-FLOW METHOD
OF THE LONGITUDINAL STABILITY CHARACTERISTICS OF A $\frac{1}{50}$ -SCALE
SEMISPAN MODEL OF THE MCDONNELL XP-88 AIRPLANE

By Harold L. Crane

SUMMARY

This paper presents the results of measurements of longitudinal stability of a $\frac{1}{50}$ -scale model of the XP-88 airplane by the wing-flow method. Lift, rolling-moment, hinge-moment, and pitching-moment characteristics as well as the downwash at the tail were measured over a Mach number range from approximately 0.5 to 1.05 at Reynolds numbers below 1,000,000. No measurements of drag were obtained.

No abrupt changes due to Mach number were noted in any of the parameters measured. The data indicated that the wing was subject to early tip stalling; that the tail effectiveness decreased gradually with increasing Mach number up to $M = 0.9$, but increased again at higher Mach numbers; that the variation of downwash with angle of attack did not change appreciably with Mach number except between 0.95 and 1.0 where $d\epsilon/d\alpha$ decreased from 0.46 to 0.32; that at zero lift with a stabilizer setting of -1.5° there was a gradually increasing nosing-up tendency with increasing Mach number; and that the control-fixed stability in maneuvers at constant speed gradually increased with increasing Mach number.

INTRODUCTION

At the request of the Air Materiel Command, U. S. Air Force, and the McDonnell Aircraft Corporation, wing-flow tests of a $\frac{1}{50}$ -scale semispan model of the XP-88 airplane have been conducted primarily to investigate the longitudinal stability characteristics at transonic speeds. The Mach number range covered in these tests was from 0.55 to 1.05.

The results of these tests which include the variation of force and moment coefficients with angle of attack and tail incidence and the variation of downwash at the tail with angle of attack for the Mach number range previously mentioned are presented herein. No measurements of drag were made. Because of the early date at which the XP-88 airplane is scheduled to fly, issuance of this paper has been expedited by including only a brief analysis and discussion of results.

APPARATUS AND TESTS

Photographs of the model in place on the test panel (a modified P-51D ammunition compartment door) are presented as figure 1. Figure 2 is a two-view drawing of the model. The model was equipped with an all-movable horizontal tail with no movable elevator. The center line of the model fuselage was bent to the curvature of the test panel to conform to the curvature of the flow along the model. Because of space limitations it was necessary to pivot the model at 55 percent of the mean aerodynamic chord.

Tests were conducted with varying angle of attack and the tail incidence near 0° . Further tests were made with the angle of attack near 0° and varying tail incidence. There was ordinarily a gap of approximately $1/64$ inch at the root of the tail. In order to investigate the effect of this gap, tail-fixed data were also obtained with this gap sealed. To obtain a separate measure of wing and tail characteristics, tests were made with tail removed. An investigation was also made of the average downwash over the tail by oscillating the model in pitch with the tail free to trim.

The tests were run at two altitude levels, 22,000 to 30,000 feet and 4000 to 8000 feet, in order to get the maximum possible range of Reynolds number, which was from 300,000 to 1,000,000. A plot of the variation of Reynolds number with Mach number for the two altitude levels is presented in figure 3.

The XP-88 model was mounted on a strain-gage balance in such a way that either the angle of attack of the model or the tail incidence could be varied through approximately 10° at a rate of approximately 1 cycle per second. This rate of oscillation amounted to a maximum of 1° per 80 chord lengths of motion with respect to the air stream and, therefore, steady flow conditions were approximated. During 1 cycle the Mach number varied a maximum of 0.02. The variation of dynamic pressure amounted to approximately 2 inches of water during a cycle, however all data were worked up in terms of the average dynamic pressure for a cycle, because no appreciable error in the coefficients resulted.

The following quantities were measured for the semispan XP-88 model: lift, pitching moment, rolling or bending moment about the model center

line, hinge moment on the all-movable tail, tail incidence, model attitude angle, and the angle of flow at the model. The angle of flow at the model with respect to the wing chord line was determined using a floating vane 22 inches outboard and a previously obtained calibration of the difference in angle of flow at the two locations.

Before installing a model, pressure surveys were made over the test panel. Typical chordwise and vertical velocity gradients are presented in figure 4. From these pressure data a chart was prepared of the variation of the average Mach number in the flow over the model wing as a function of airplane Mach number and lift coefficient. In the workup of data this chart was used to determine Mach number at the model which in turn was used to determine the dynamic pressure at the model.

ACCURACY

A table of approximate probable errors in the various measured quantities is presented below. Errors in absolute values and in increments of the specified variable read from faired curves during one series of tests for one configuration and/or Reynolds number range are presented.

	<u>Error</u>	<u>Error in increment</u>
Mach number, M	0.01	----
Dynamic pressure, q_0 , percent	1	----
Angle of attack, α , degrees	0.4	0.1
Tail incidence, i_t , degrees	0.2	0.05
Downwash angle, ϵ , degrees	0.5	0.1
Lift, L, pounds	0.5	0.2
Pitching moment, M, inch-pounds	0.5	0.2
Rolling moment, L' , inch-pounds	1	0.4
Hinge moment, H, inch-pounds	0.1	0.05

The possible errors noted do not take into account the effects of the velocity gradients over the model.

RESULTS

Typical Data

A view of a galvanometer record and a typical plot of the data obtained as they were first worked up are presented in figure 5. Figure 5(b) presents the variation of the coefficients of lift C_L ,

pitching moment C_m , and tail hinge moment C_h with angle of attack for a tail incidence of -1.5° and a Mach number of 1.00. No determination of rolling-moment coefficient C_l was made in this case. The irregularities in the pitching-moment record were introduced by the driving mechanism and are not to be interpreted as buffeting. It was possible to correct for the moment introduced by the actuator because it was a function of the model angle. The force and moment coefficients were determined from the following expressions:

$$C_L = \frac{L}{q_o S}$$

$$C_l = \frac{L'}{q_o S b}$$

$$C_m = \frac{M}{q_o S \bar{c}} \quad (\text{about 55 percent } \bar{c})$$

$$C_h = \frac{H}{q_o S_t \bar{c}_t}$$

in which

- q_o dynamic pressure, pounds per square foot $\left(\frac{1}{2}\rho V^2\right)$
 S wing area of semispan model, square feet
 \bar{c} wing mean aerodynamic chord, feet
 S_t horizontal-tail area of semispan model, square feet
 \bar{c}_t tail mean aerodynamic chord, feet
 b wing span of semispan model, feet

Tail Off

The variations of lift coefficient, pitching-moment coefficient, and rolling-moment coefficient with angle of attack from the wing chord line at various Mach numbers throughout the test range are presented in figure 6 for the two Reynolds number ranges. In figure 6 and subsequent figures the symbols are used for identification and do not represent test points. An early tip stall is evident from an examination of the plots of C_l against α . Because of the very low Reynolds number of these tests this tip stalling occurs at a very low angle of attack at the lower Mach numbers.

The variations of the slopes $C_{L\alpha}$, $C_{m\alpha}$, and $C_{l\alpha}$ and the longitudinal stability derivative dC_m/dC_L , measured near 0° angle of attack, with Mach number are shown in figure 7. The slope of the lift curve increased from approximately 0.06 to nearly 0.08 at $M = 0.9$ and then decreased gradually. The value of $C_{m\alpha}$ remained fairly constant up to $M = 0.8$ and then gradually became less positive indicating increasing stability. (Pivot axis, 55 percent \bar{c} .) The variation of the stability derivative dC_m/dC_L was similar to that of $C_{m\alpha}$, and the variation of $C_{l\alpha}$ was similar to that of $C_{L\alpha}$.

Tail On and Fixed

The variations with angle of attack of C_L , C_m , and C_h , the hinge-moment coefficient for the all-movable horizontal tail, are presented in figure 8 for various Mach numbers throughout the test range. The hinge moments on the tail are presented in terms of the pivot axis 3 percent of the mean aerodynamic chord ahead of the leading edge at the mean aerodynamic chord of the tail. The tail incidence was -1.5° with respect to the wing chord line. Figure 9 shows the variation of C_L and C_m with α with the tail gap sealed. These data show a decrease in stability at high angles of attack due to tip stalling. The data also show that at zero lift there was a nosing-up tendency with increasing Mach number.

The variation of the slopes $C_{L\alpha}$, $C_{m\alpha}$, and $C_{h\alpha}$ and the longitudinal stability derivative dC_m/dC_L , measured near 0° , with Mach number with tail on and held fixed are given in figure 10. These data show that there were no abrupt changes in stability characteristics as the Mach number was increased. The aerodynamic center moved from approximately 45 to 60 percent of the mean aerodynamic chord with increasing Mach number. Comparison with figure 7 shows that the contribution of the horizontal tail to longitudinal stability did not vary

appreciably with Mach number. The data also show that sealing the gap at the tail root caused an appreciable increase in stability.

Tail Oscillating

The variations of lift coefficient, pitching-moment coefficient, and hinge-moment coefficient with tail incidence at Mach numbers throughout the test range and for the two Reynolds number ranges are presented in figure 11. The angle of attack was approximately 0° for all the data of figure 11 and was constant for the data at any Mach number. Why these data have different slopes on either side of zero incidence is not clear. The hinge-moment data is subject to some question because the angles of tail incidence for zero hinge moment appear to be in error.

The variation of the slopes $C_{L_{it}}$, $C_{m_{it}}$, and $C_{h_{it}}$ with Mach number are presented in figure 12. Because of the nonlinearity of the curves these slopes were measured as the average slopes over the deflection range tested. These data indicate a gradual decrease in tail effectiveness up to $M = 0.9$ followed by an increase at higher Mach numbers. The Reynolds number effect is rather large for these data.

Downwash Determination

Data were obtained with the tail free to trim while the model oscillated in pitch. Figure 13 shows the variation of tail incidence for trim at zero hinge moment with angle of attack for Mach numbers throughout the test range and for the two Reynolds number ranges. These data show a large increase in rate of change of downwash over the tail with angle of attack at the angles of attack where tip stalling of the wing occurs.

Figure 14 shows the variation with Mach number of the downwash factor $d\epsilon/d\alpha$ for flow at the tail at small angles of attack for the two ranges of Reynolds number. The value of $d\epsilon/d\alpha$ was approximately constant at 0.45 up to $M = 0.95$ and then decreased to approximately 0.3 at $M = 1.0$. From $M = 1.0$ to 1.1 $d\epsilon/d\alpha$ was almost constant.

CONCLUSIONS

The principal conclusions from the wing-flow tests of the longitudinal stability of the XP-88 airplane were as follows:

1. There was slight decrease in lift-curve slope above a Mach number of approximately 0.9.

2. At zero lift with a tail setting of -1.5° there was a nosing-up tendency with increasing Mach number.

3. The control-fixed stability in maneuvers at constant velocity became greater at Mach numbers above approximately 0.85 with the aerodynamic center moving gradually from about 45 to 60 percent mean aerodynamic chord.

4. The model was subject to early tip stalling of the wings which was accompanied by a large increase in rate of change of downwash over the tail with angle of attack.

5. The rate of change of the downwash at the tail with angle of attack $d\epsilon/d\alpha$ for small angles of attack was approximately constant at 0.45 up to $M = 0.95$. Between $M = 0.95$ and $M = 1.0$ the value decreased to approximately 0.3 and then remained constant to $M = 1.1$.

6. The horizontal-tail effectiveness in terms of $C_{m_{it}}$ decreased gradually with increasing Mach numbers up to $M = 0.9$ and then gradually increased at higher Mach numbers.

Langley Memorial Aeronautical Laboratory
National Advisory Committee for Aeronautics
Langley Field, Va.

Harold L. Crane

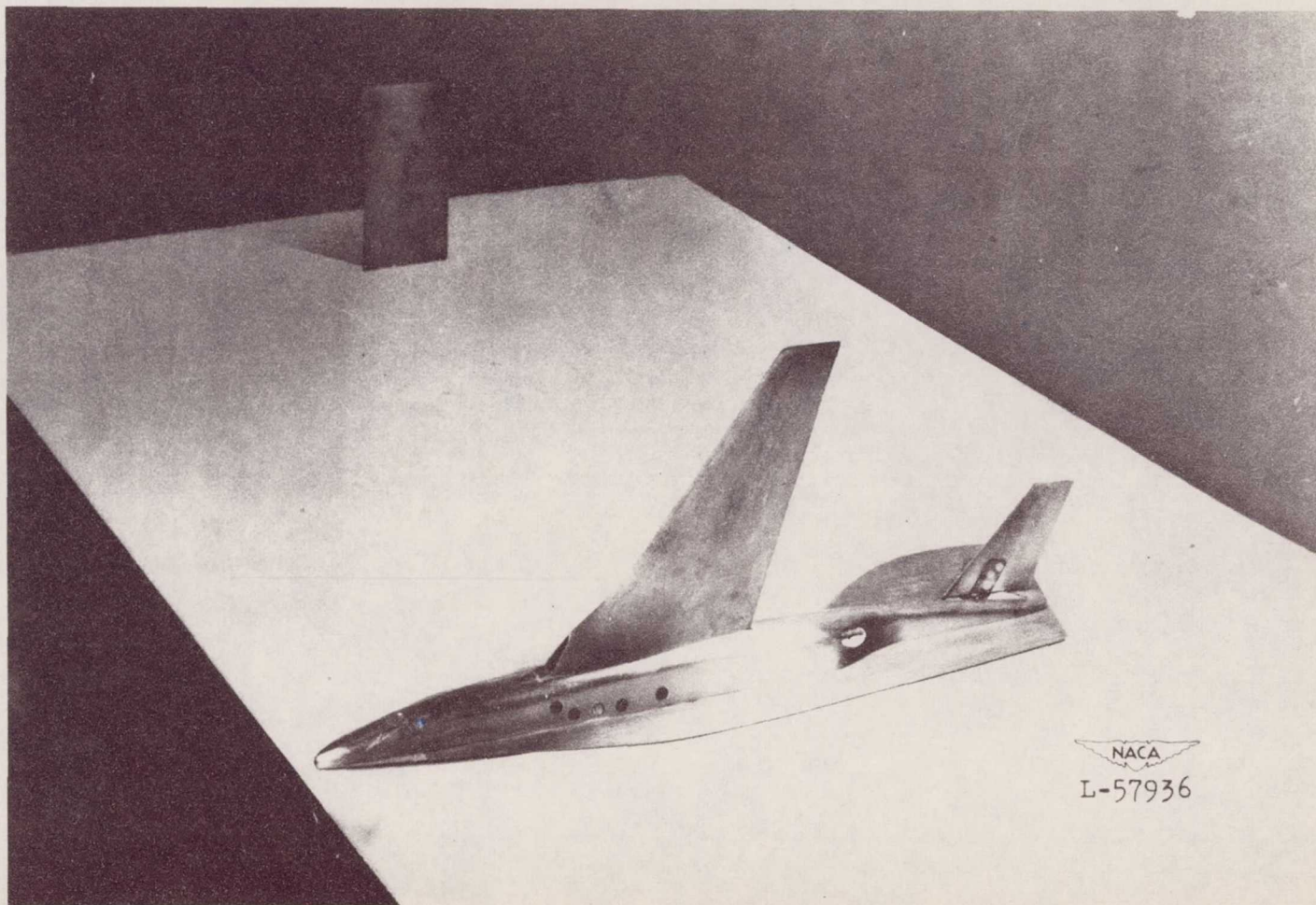
Harold L. Crane
Aeronautical Research Scientist

Approved:

J. W. Wetmore
for Melvin N. Gough
Chief of Flight Research Division

bkb

CONFIDENTIAL



NACA RM No. SL8E28a

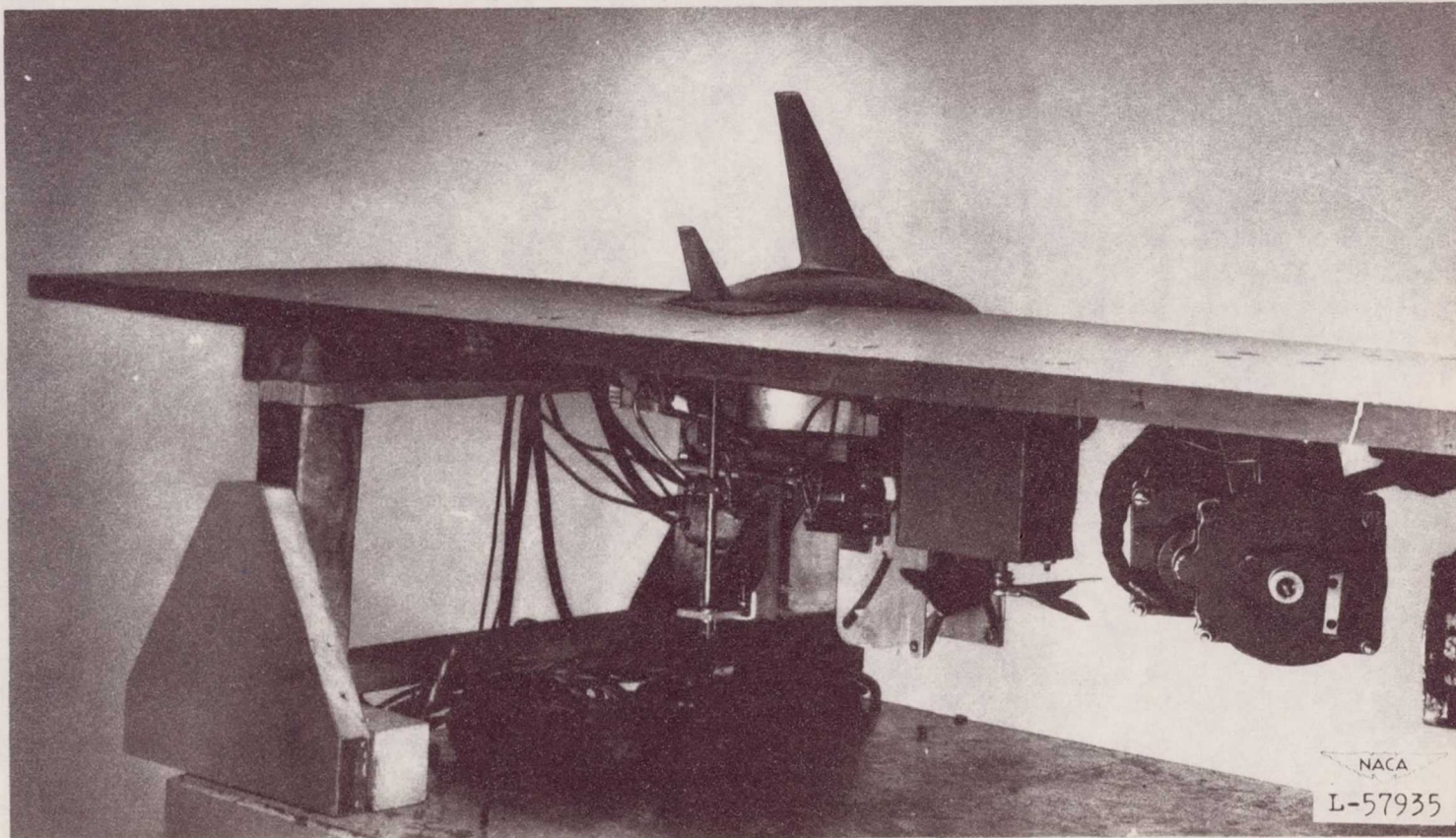
(a) Oblique view showing flow-direction vane.

Figure 1.- Photographs of $\frac{1}{50}$ -scale semispan wing-flow model of the XP-88 airplane.

CONFIDENTIAL

CONFIDENTIAL

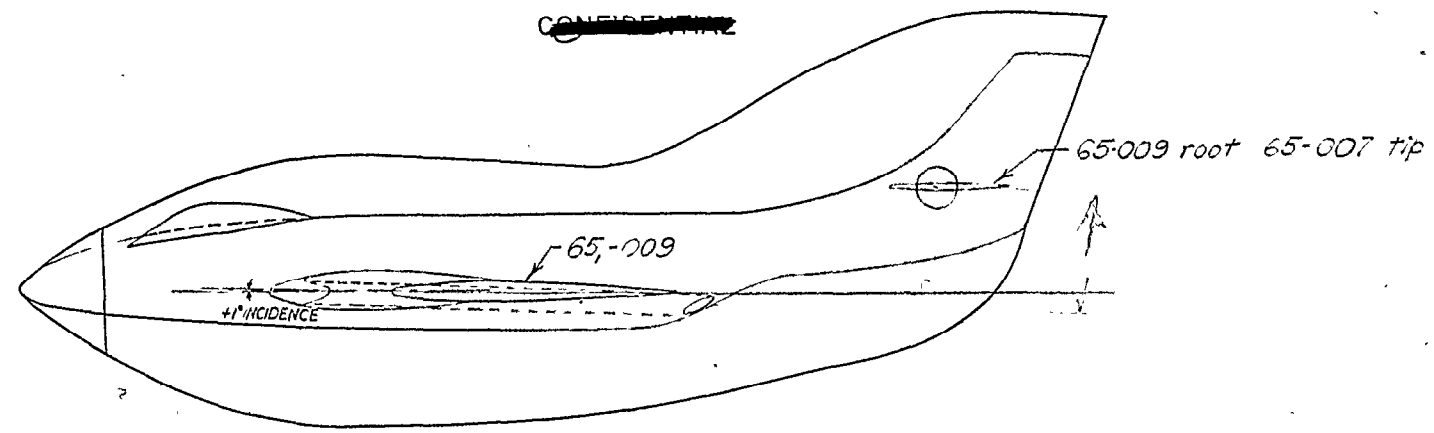
NACA RM No. SL8E28a



(b) General view including balance.

Figure 1.- Concluded.

CONFIDENTIAL



$S = 10.1 \text{ sq in.}$
 $S_t = 2.1 \text{ sq in.}$
 $\bar{x} = 2.35 \text{ in.}$
 $\bar{x}_t = 1.17 \text{ in.}$

$\frac{1}{50} \times 10.1 = .202$
 $\frac{1}{50} \times 2.1 = .042$
 $\frac{1}{50} \times 2.35 = .047$
 $\frac{1}{50} \times 1.17 = .0234$

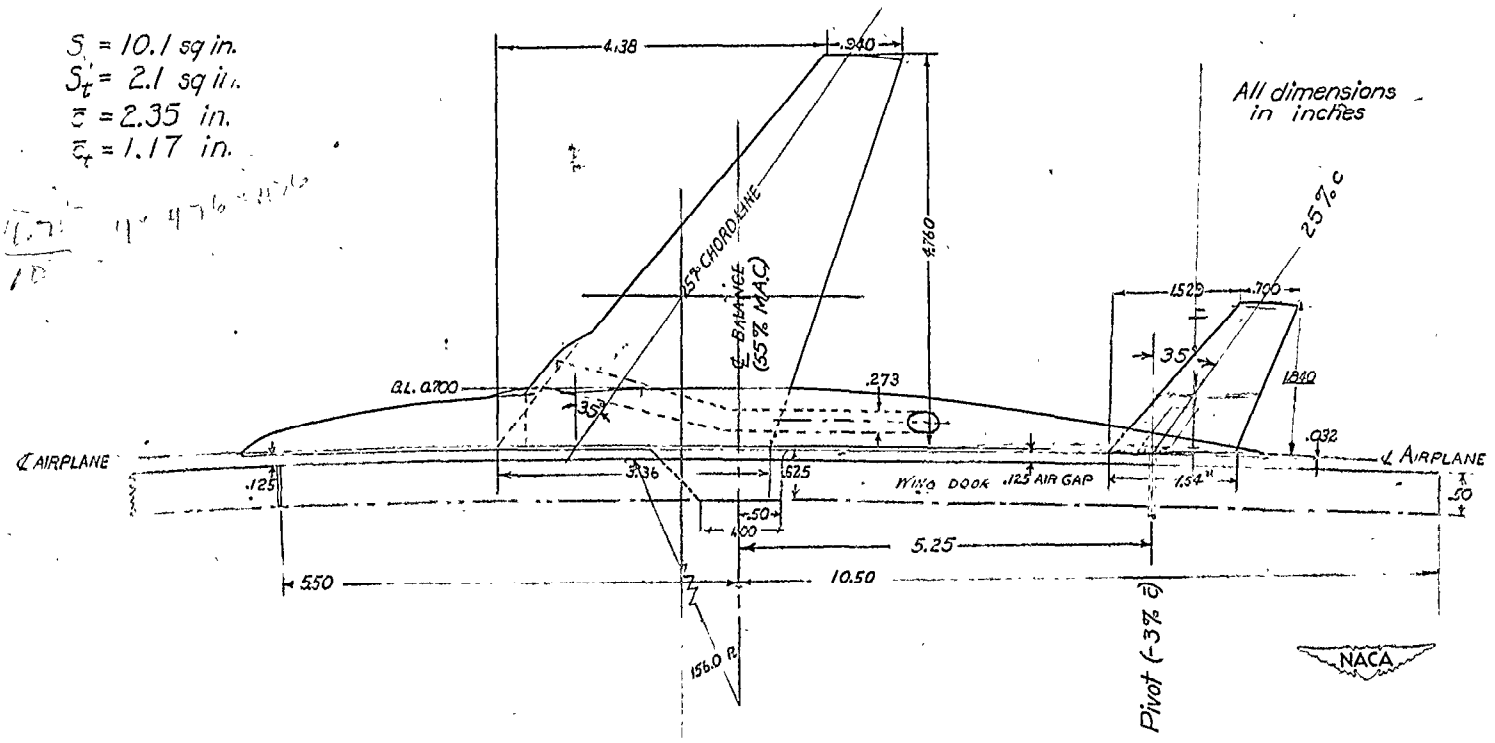


Figure 2.- Drawing of $\frac{1}{50}$ -scale wing-flow model of XP-88 airplane.

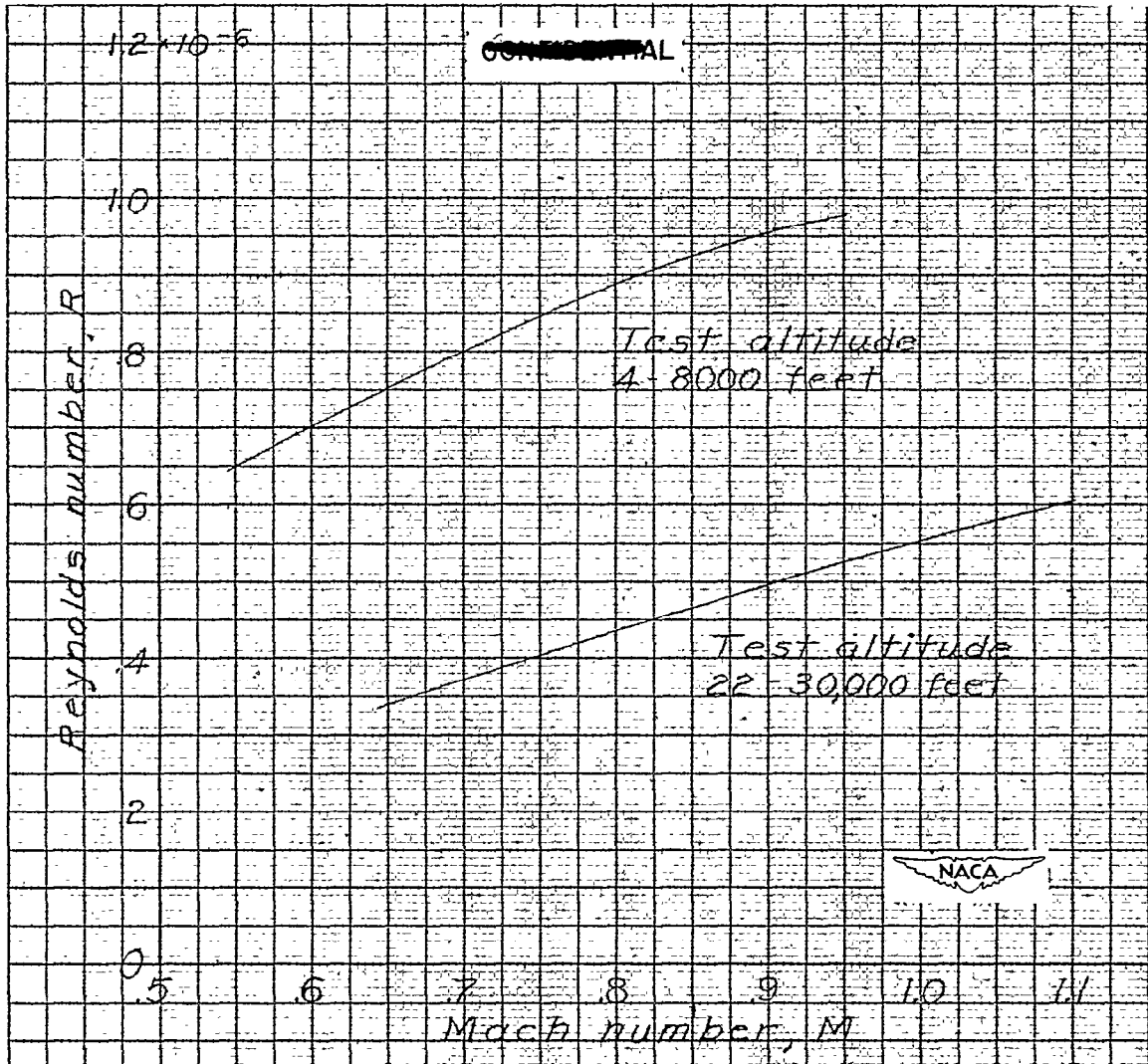
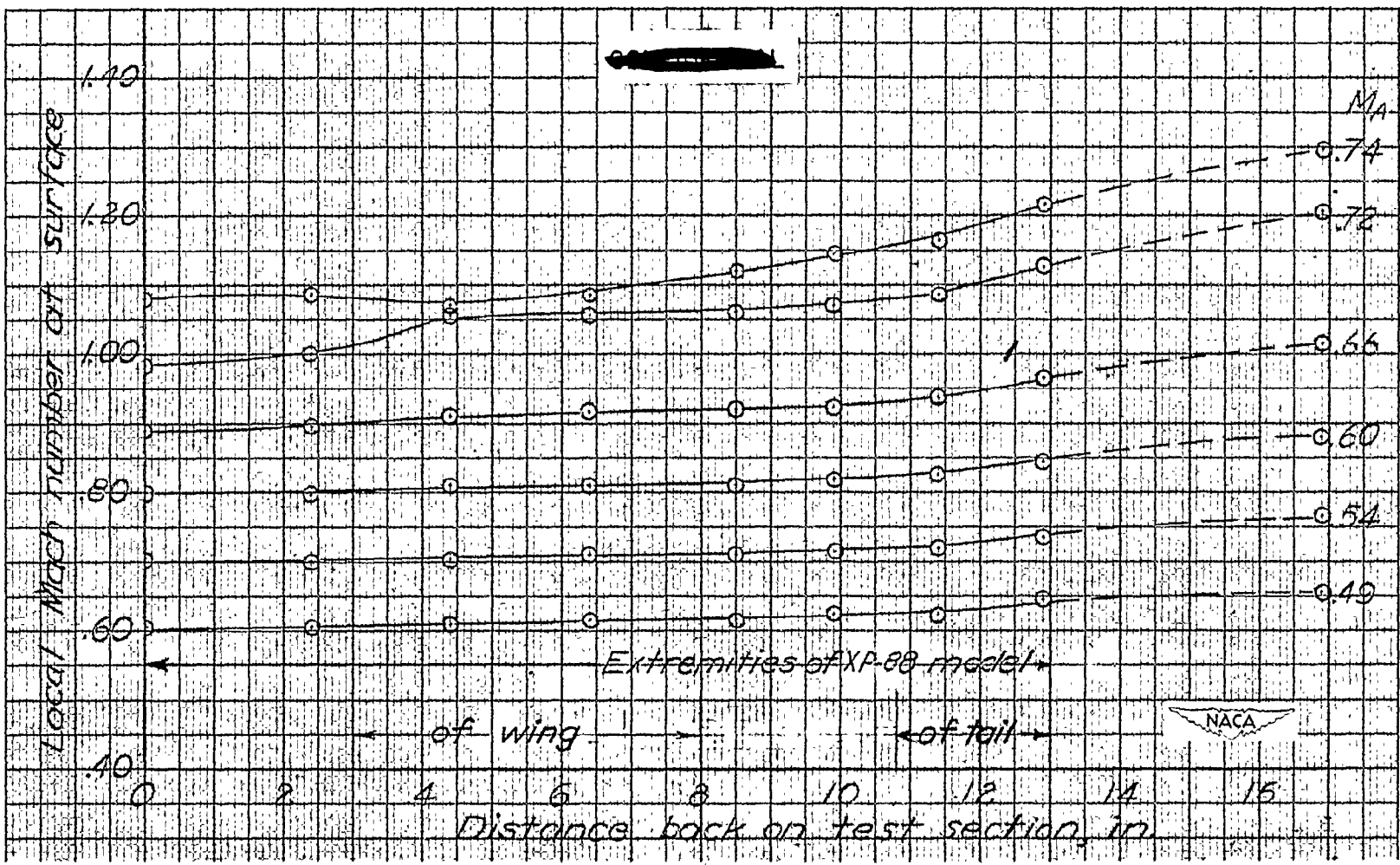


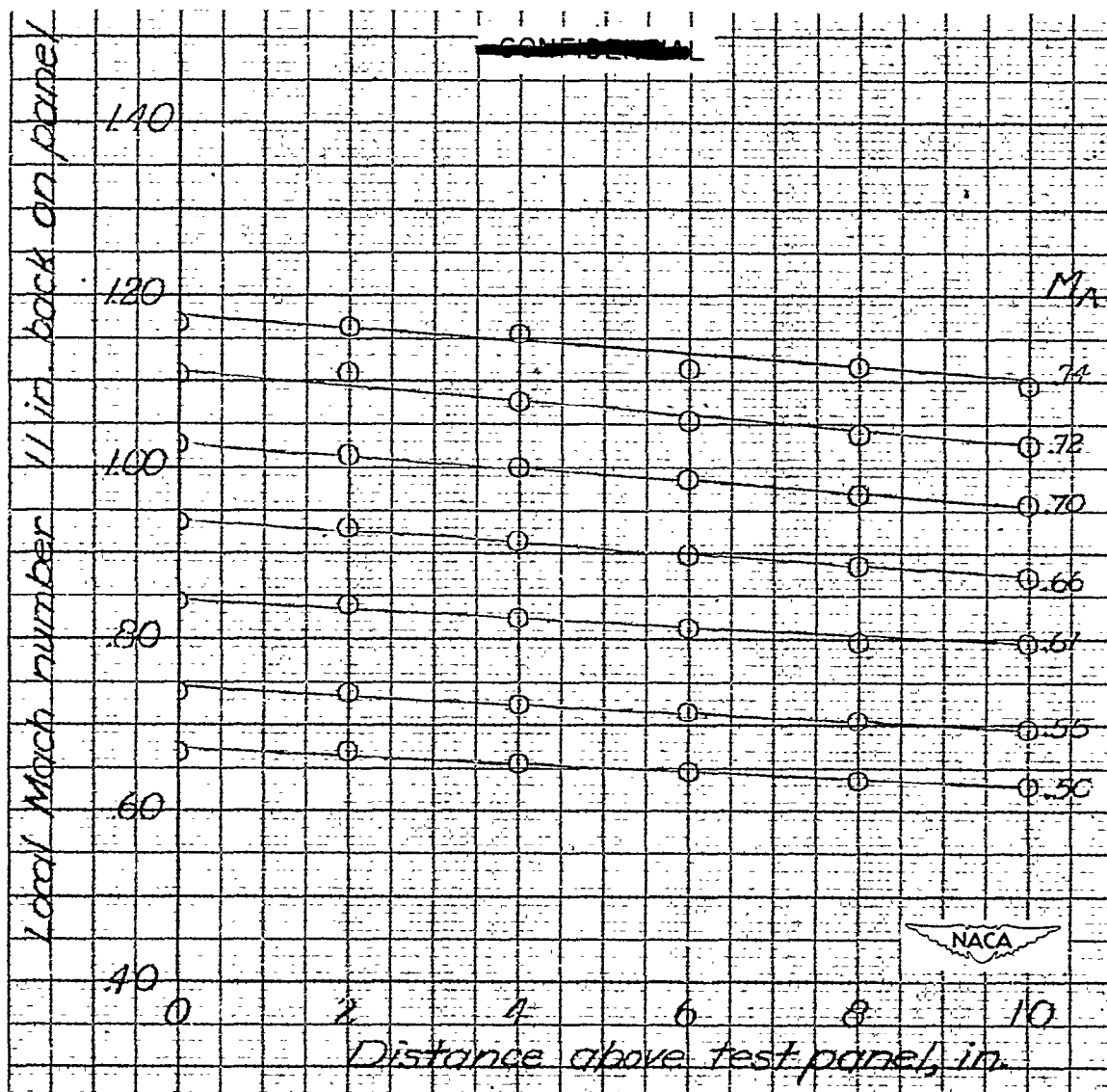
Figure 3.- Variation of Reynolds number based on the mean aerodynamic chord of the wing with Mach number during test runs at altitude levels.



(a) Typical chordwise gradient.

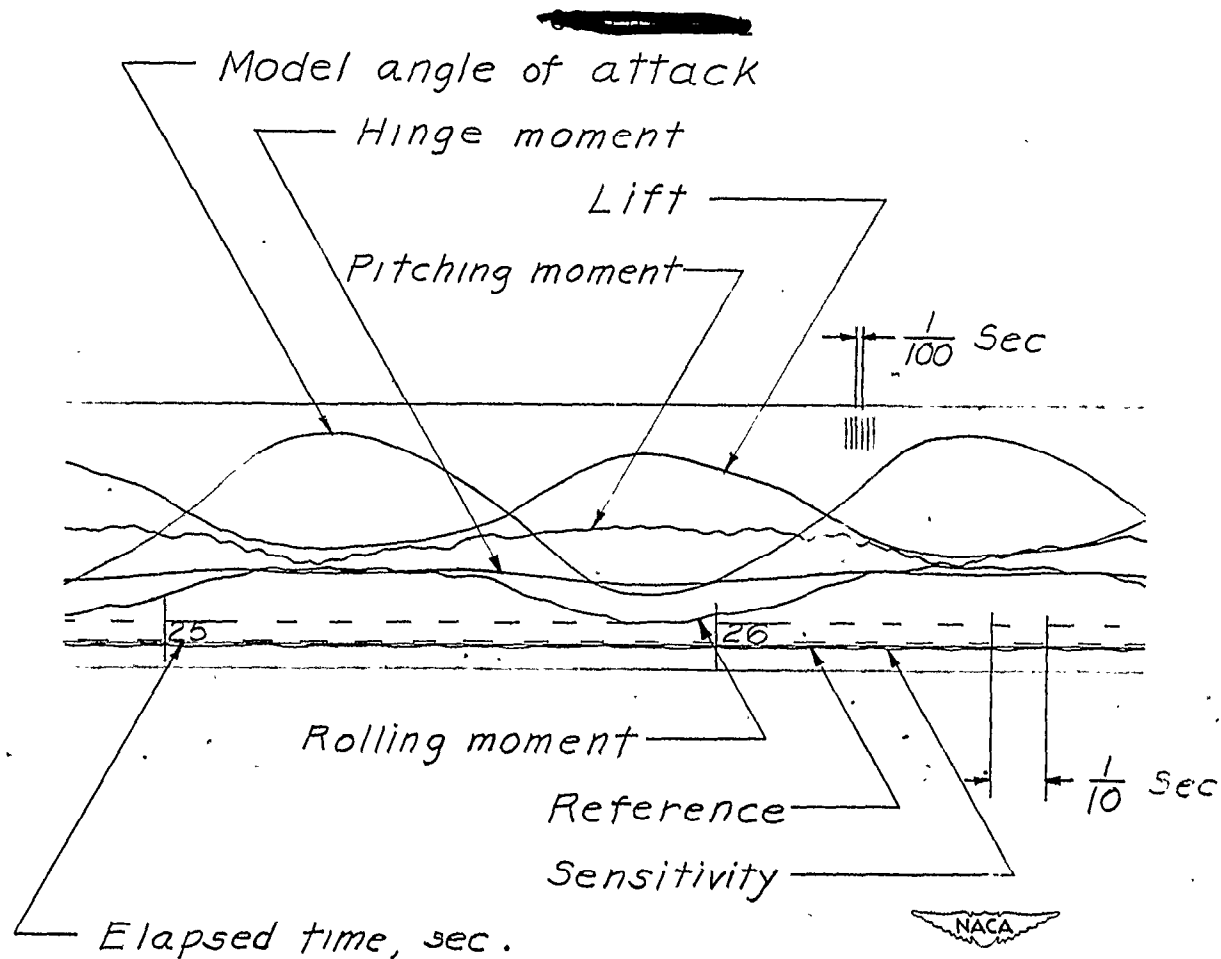
Figure 4.- Local Mach number gradients at test section for various values of airplane Mach number M_A .

~~CONFIDENTIAL~~



(b) Typical vertical gradient.

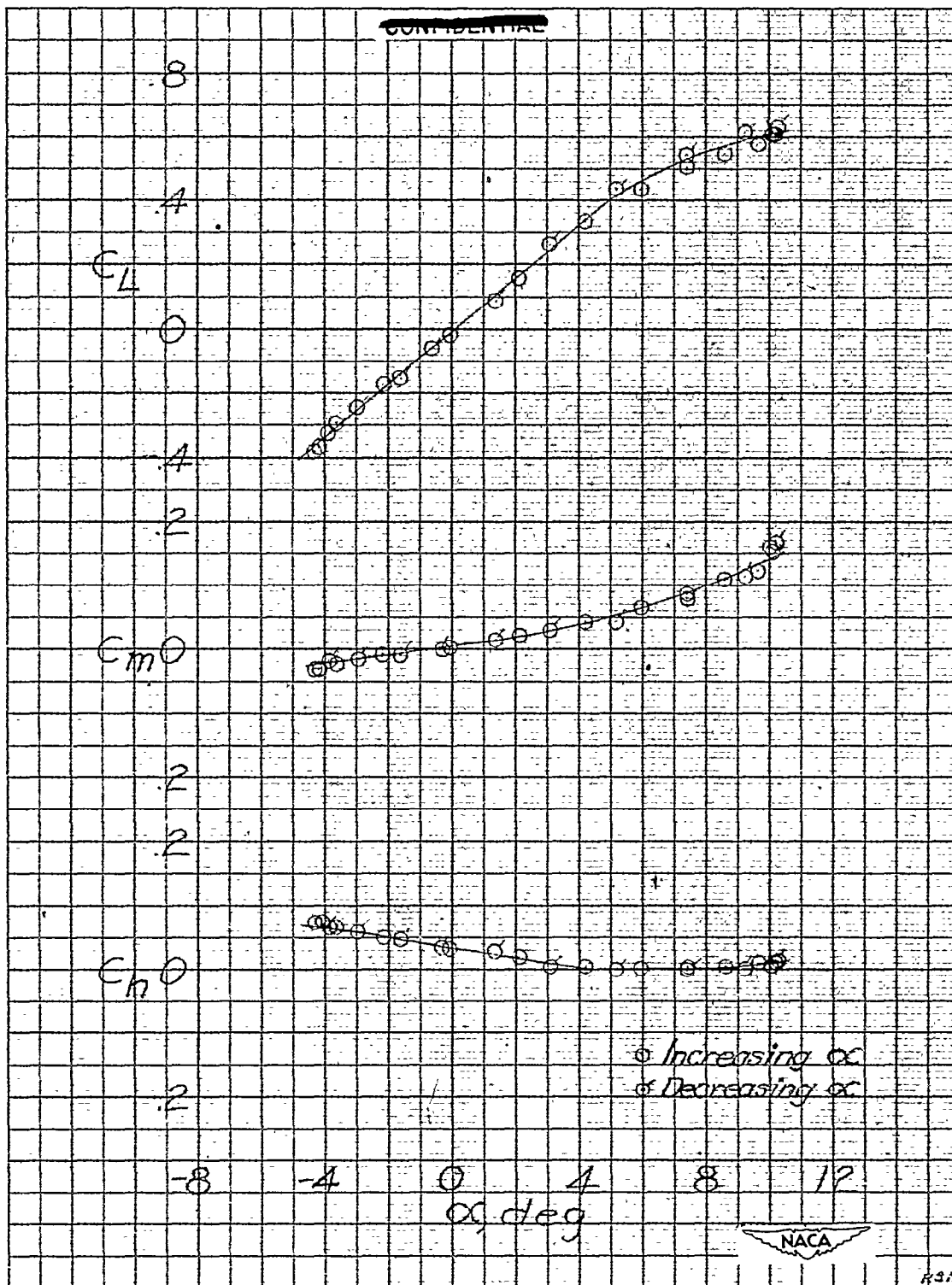
Figure 4.- Concluded.



(a) Continuous record from galvanometer.

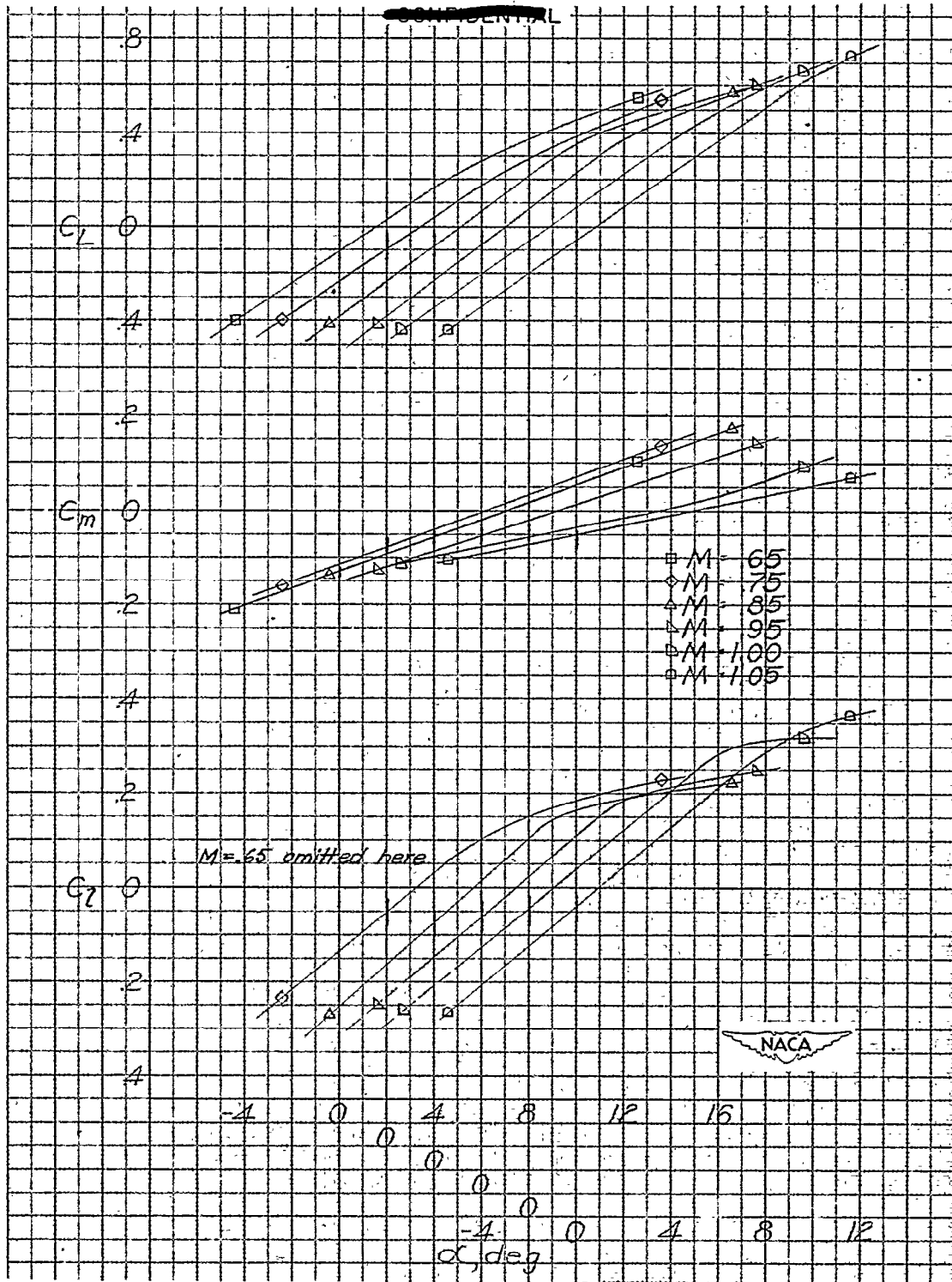
Figure 5.- Typical data as first obtained. Mach number of 1.00 and a tail setting of -1.5° with respect to wing chord line; XP-88 wing-flow model.

CONFIDENTIAL



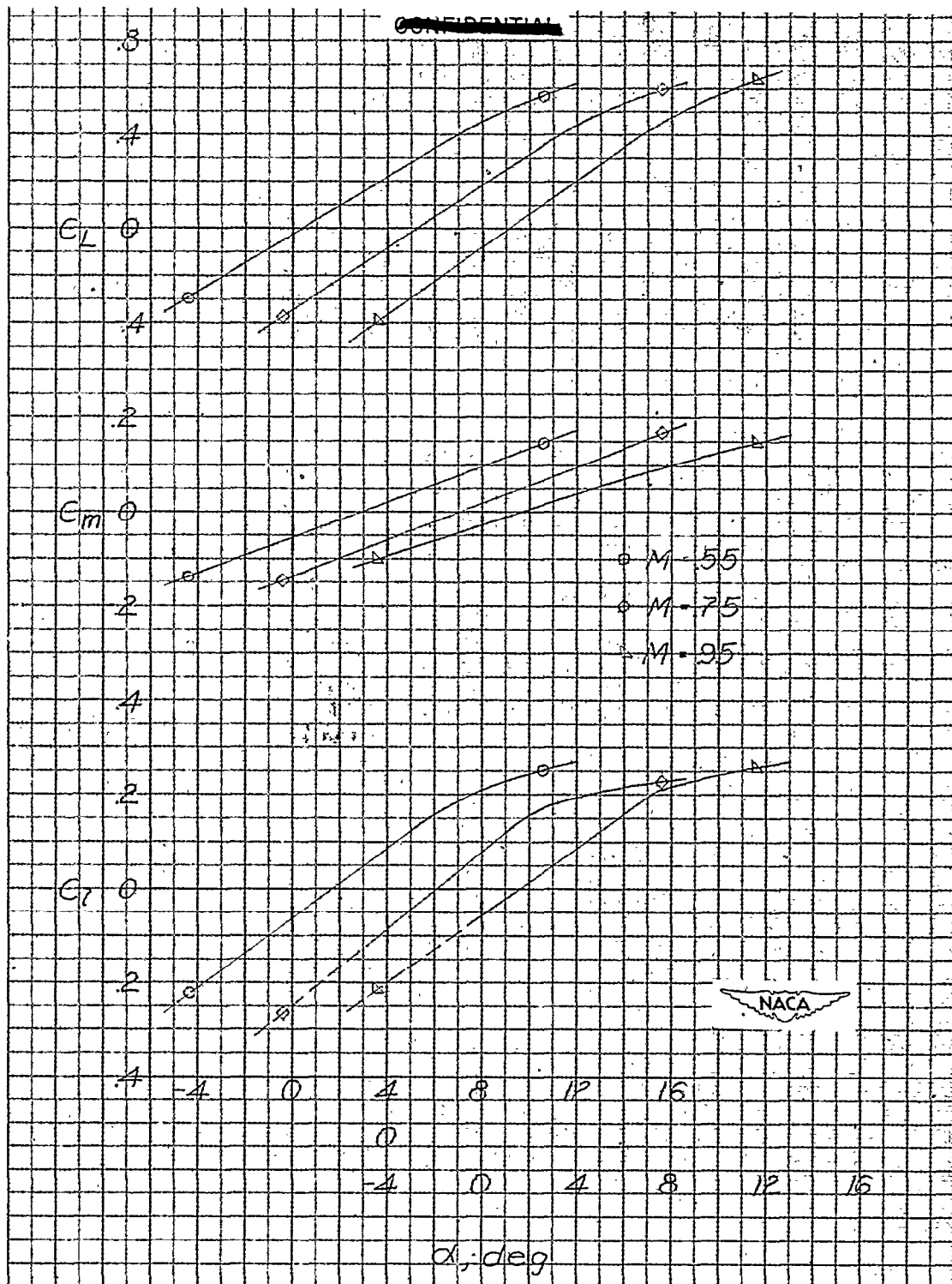
(b) Data as first plotted.

Figure 5.- Concluded.



(a) Reynolds numbers from 300,000 to 600,000.

Figure 6.- Variation of coefficients of lift, pitching moment, about 55-percent \bar{c} , and rolling moment with angle of attack at Mach numbers throughout test range. XP-88 wing-flow model with tail removed.



(b) Reynolds numbers from 600,000 to 1,000,000.

Figure 6.- Concluded.

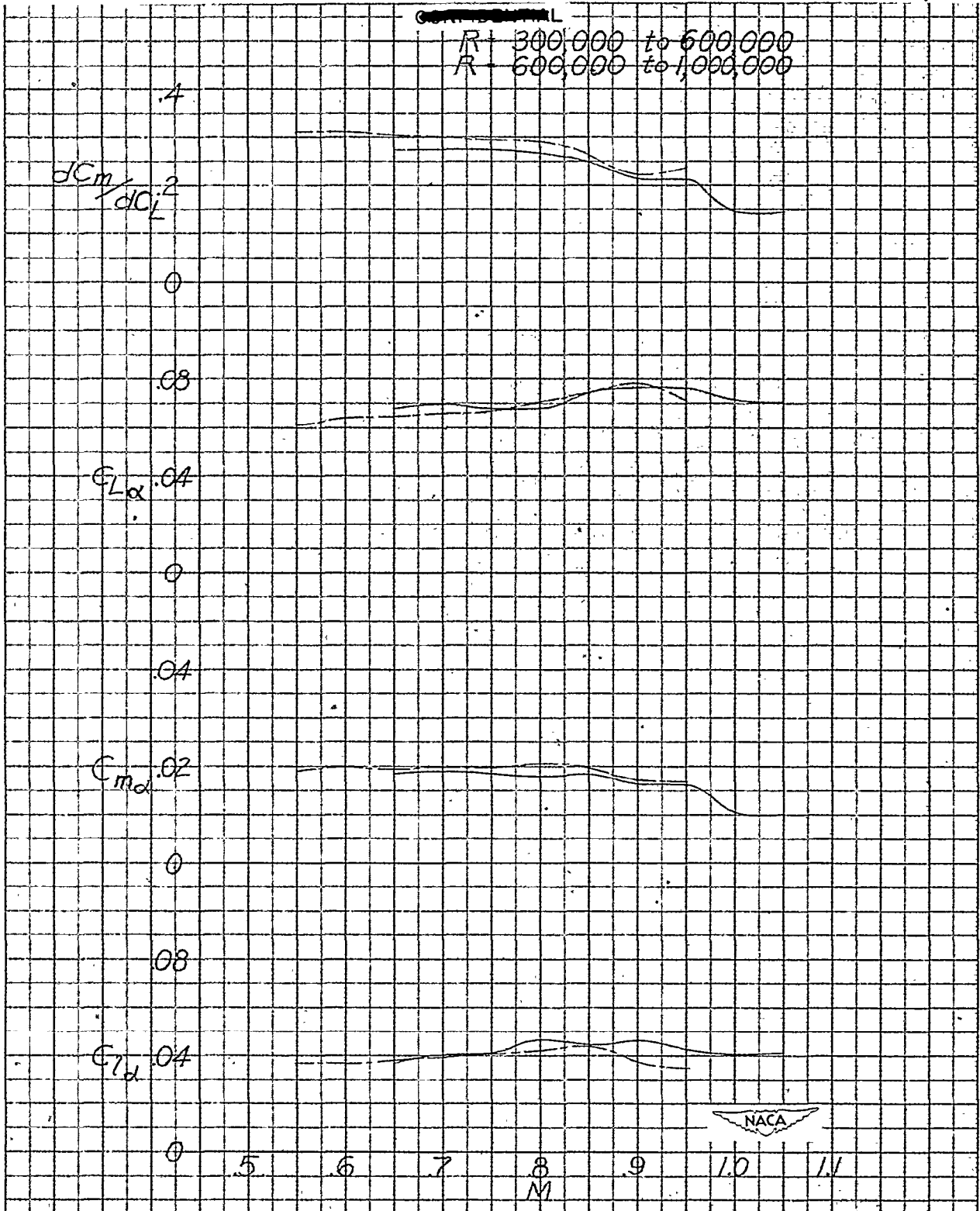


Figure 7.- Variation of $C_{L\alpha}$, $C_{m\alpha}$, $C_{L\alpha}$, and dC_m/dC_L with Mach number for two ranges of Reynolds number, XP-88 wing-flow model with tail removed.

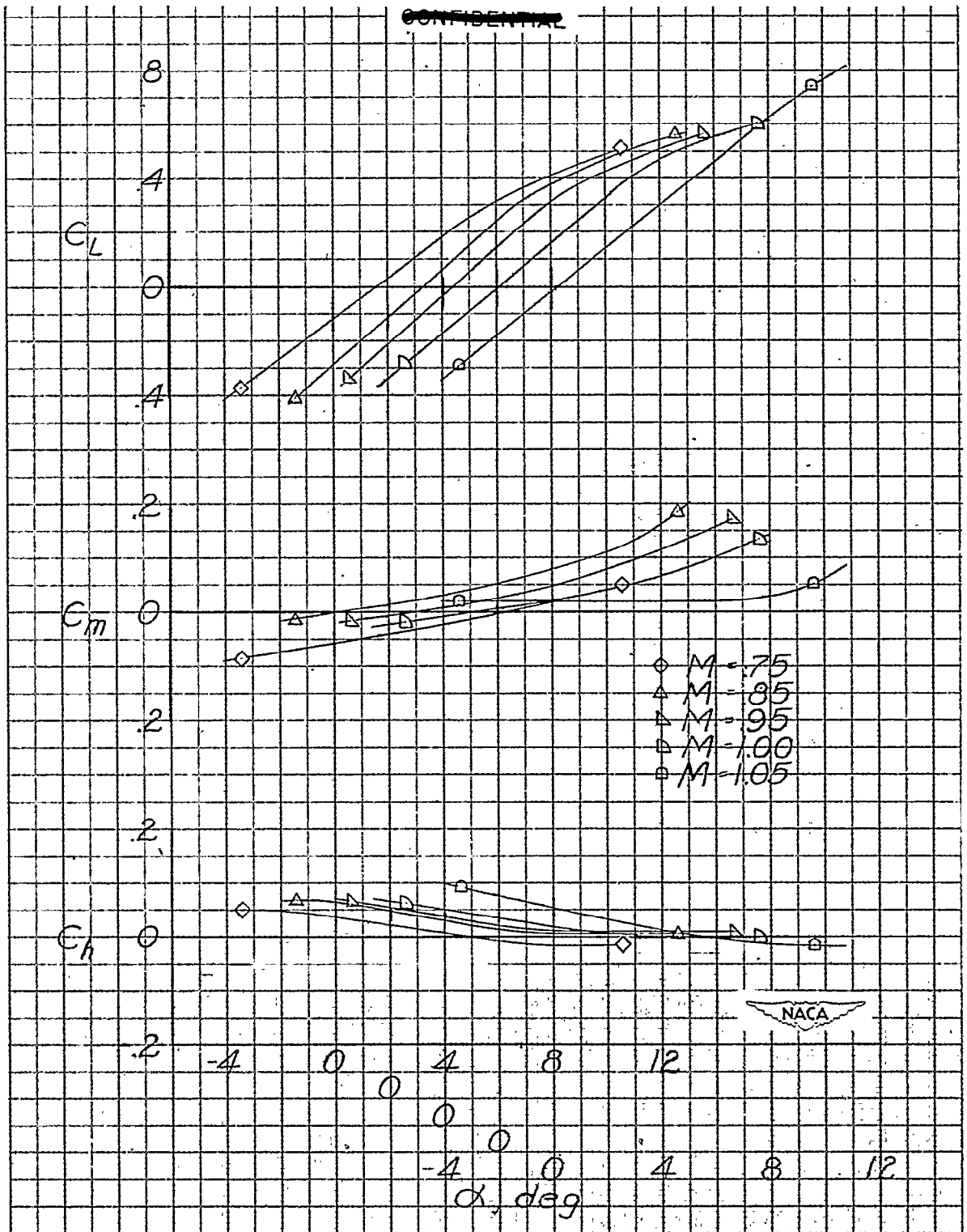
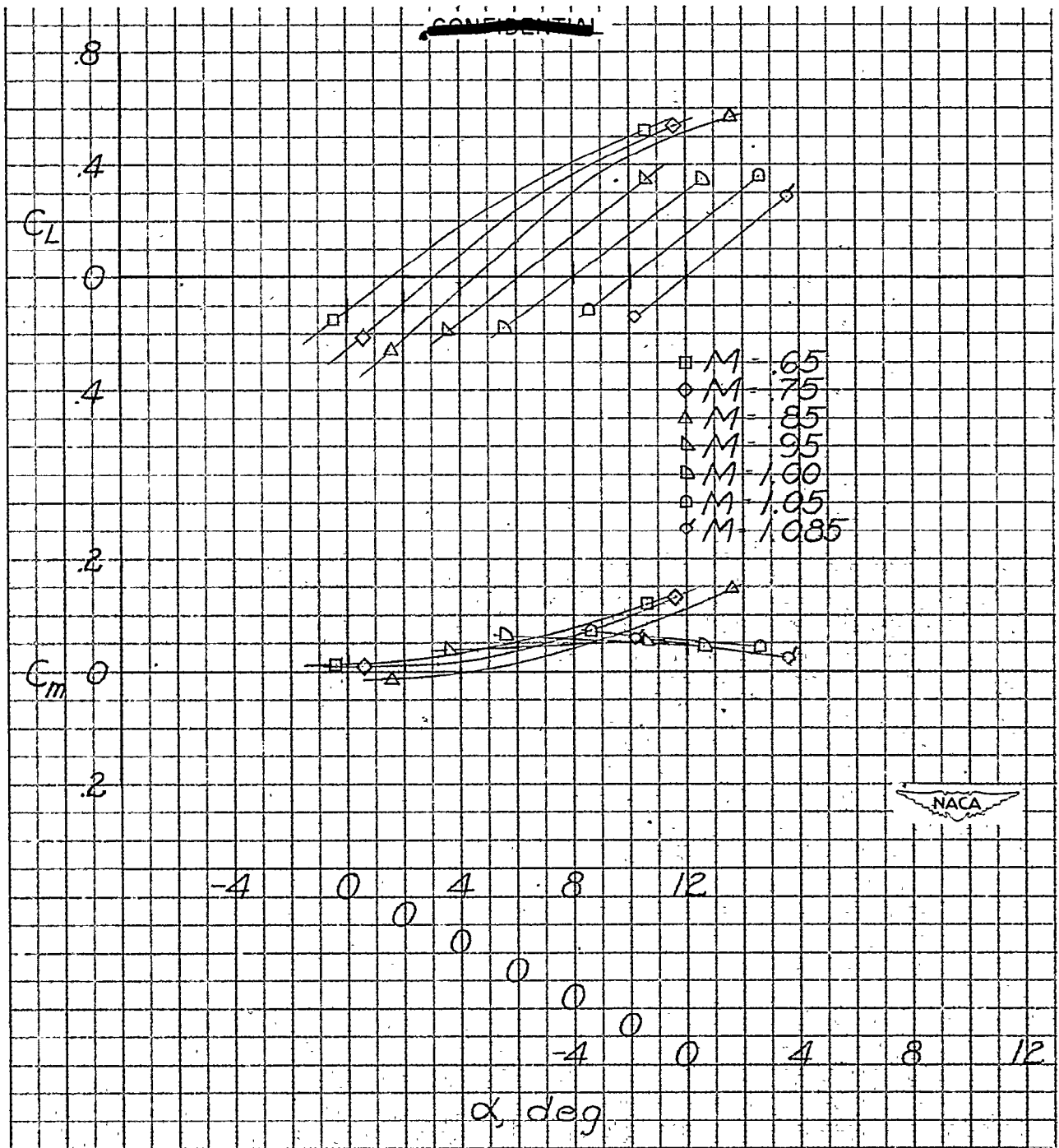
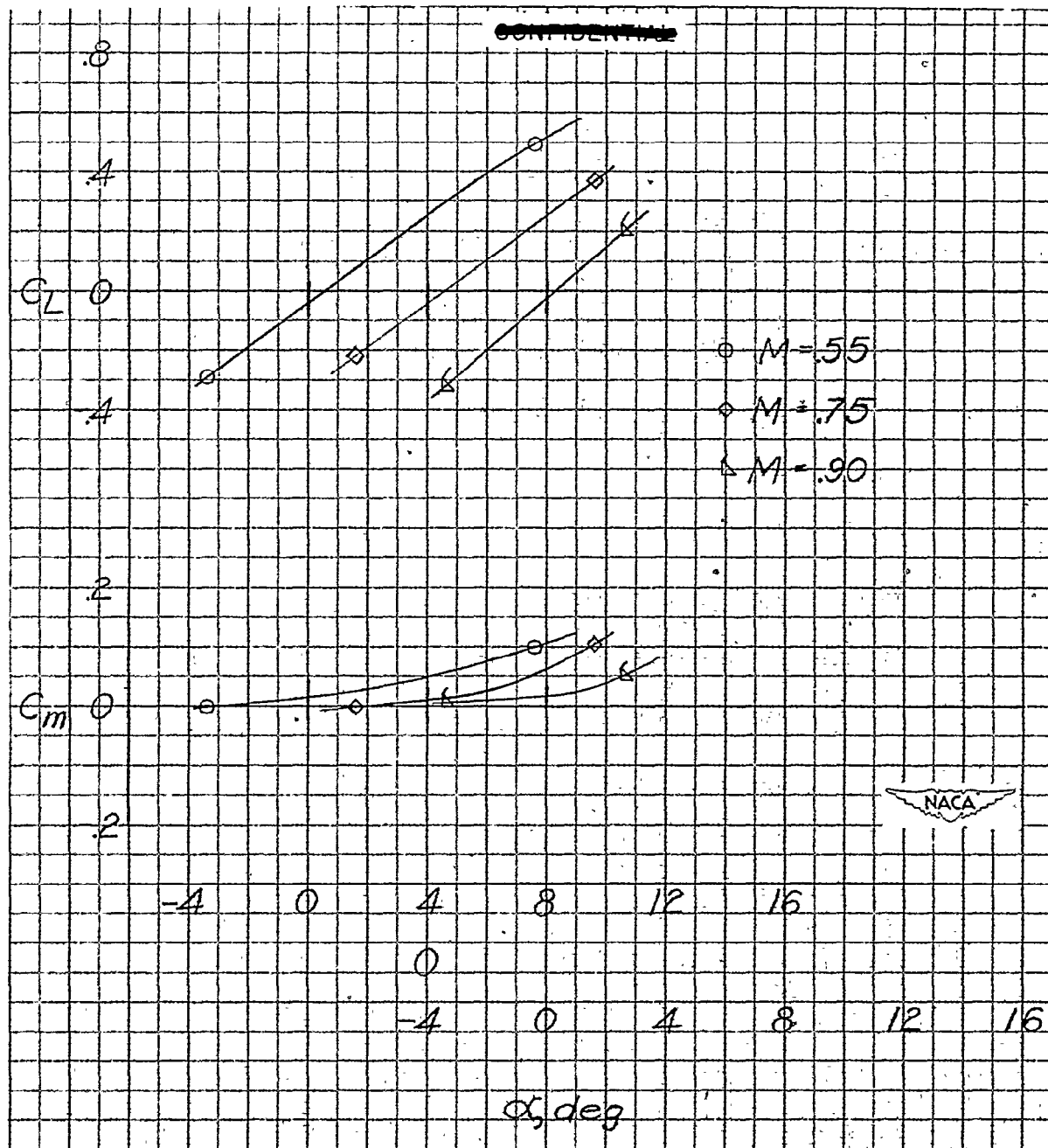


Figure 8.- Variation of coefficients of lift, pitching moment, about 55-percent \bar{c} , and hinge moment with angle of attack at Mach numbers throughout test range, XP-88 wing-flow model with tail set at -1.5° with respect to wing chord line, tail gap unsealed, Reynolds numbers from 300,000 to 600,000.



(a) Reynolds numbers from 300,000 to 600,000.

Figure 9.- Variation of coefficients of lift and pitching moment, about 55-percent \bar{c} , with angle of attack at Mach numbers throughout the test range, XP-88 wing-flow model with tail set at -1.5° and gap sealed.



(b) Reynolds numbers from 600,000 to 1,000,000.

Figure 9.- Concluded.

~~CONFIDENTIAL~~

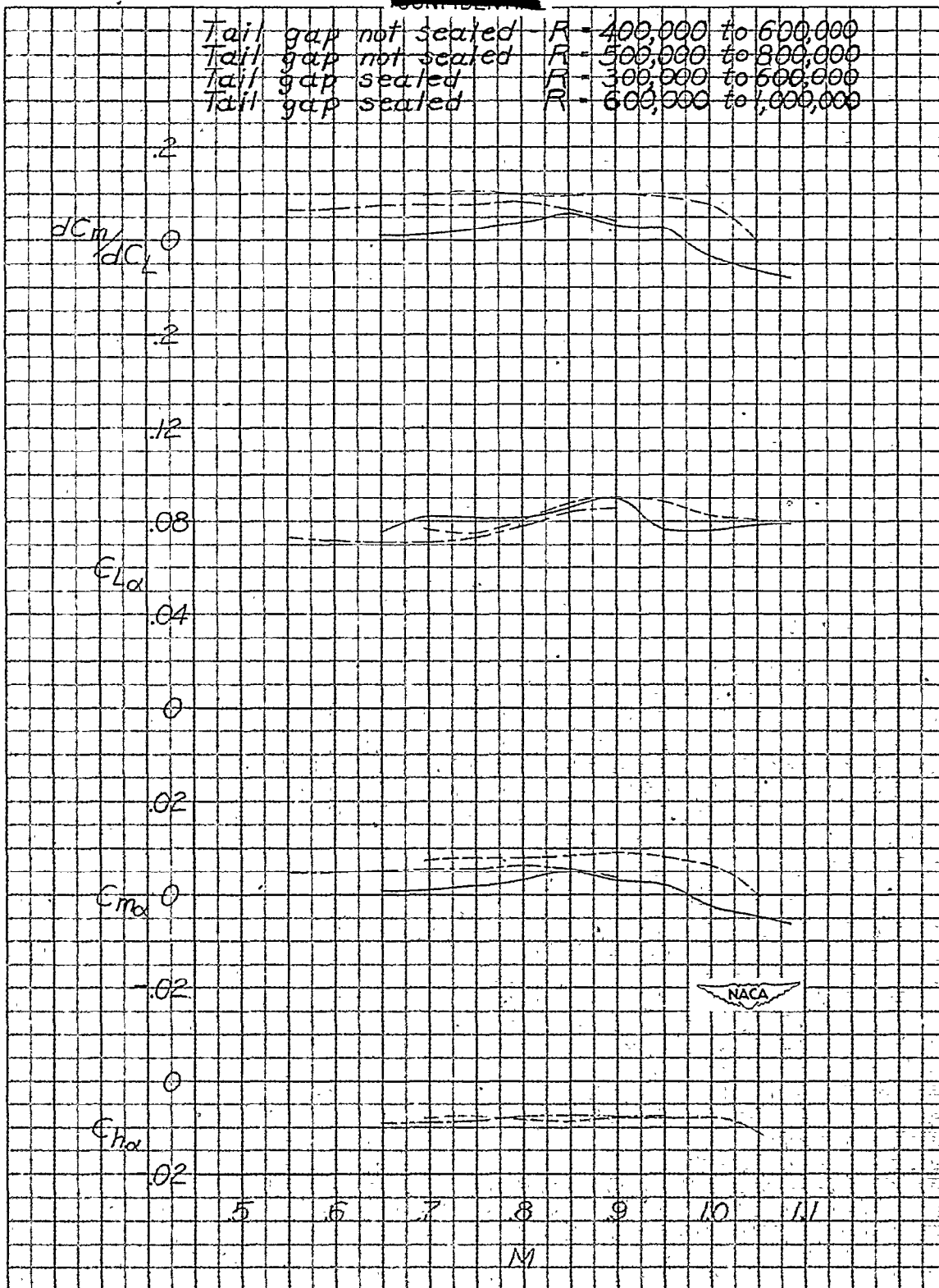
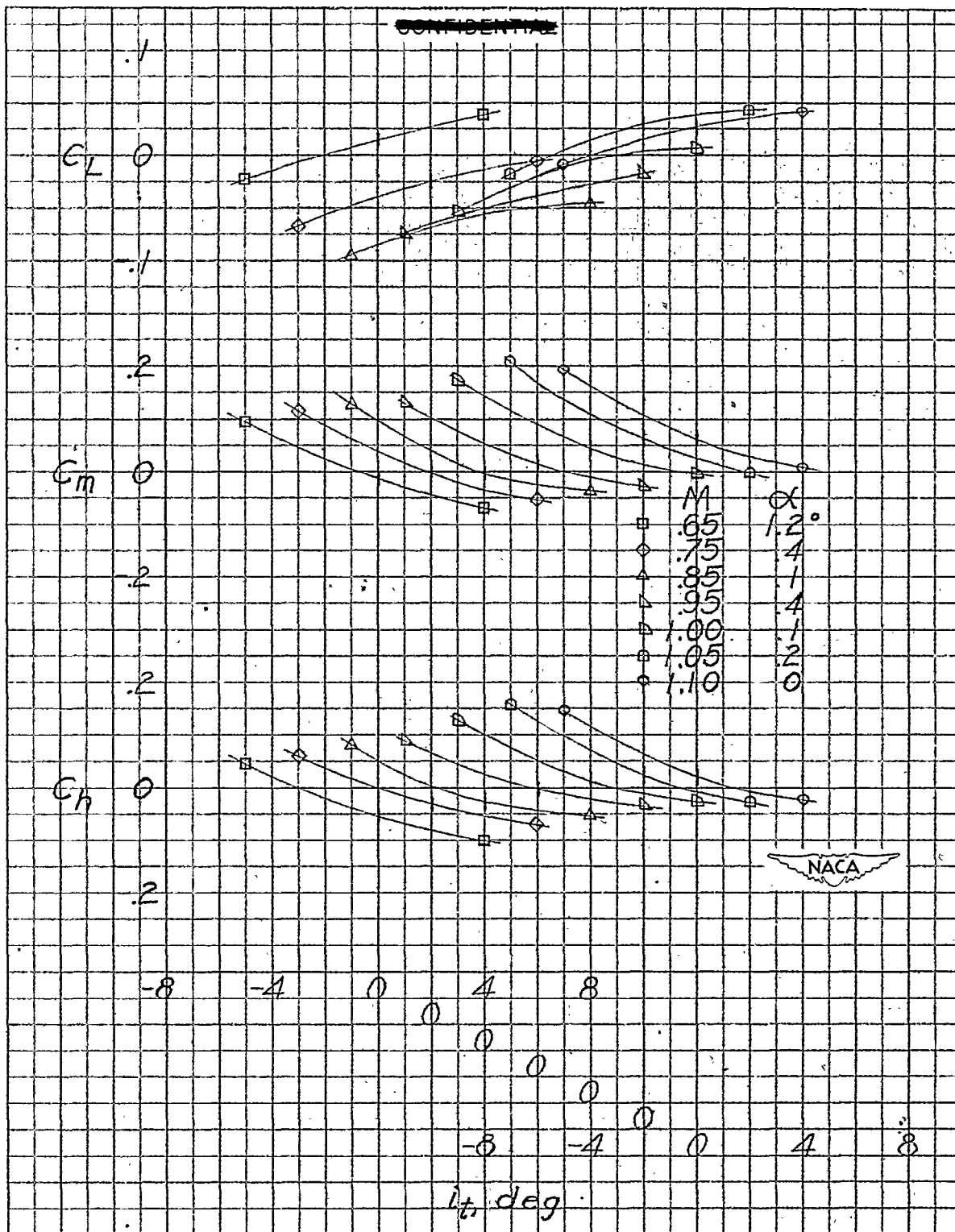


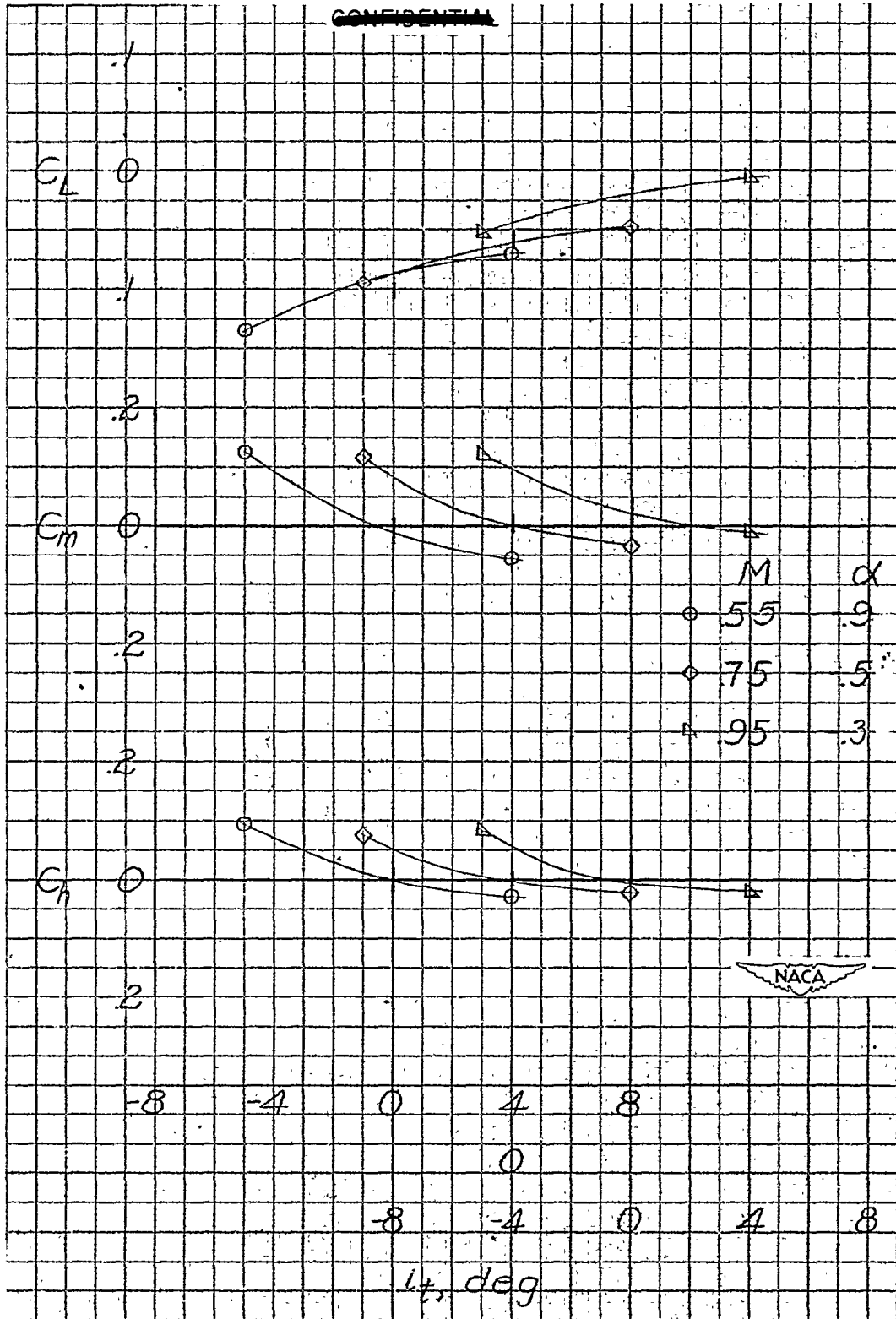
Figure 10.- Variation of C_{L_α} , C_{m_α} , C_{l_α} , C_{h_α} , and dC_m/dC_L with Mach number for two ranges of Reynolds number, XP-88 wing-flow model with tail at -1.5° with gap sealed and unsealed.

~~CONFIDENTIAL~~



(a) Reynolds numbers from 150,000 to 300,000 based on mean aerodynamic chord of tail.

Figure 11.- Variation of coefficients of lift, pitching moment, about 55-percent \bar{c} , and hinge moment with tail incidence at Mach numbers throughout the test range. XP-88 wing-flow model.



(b) Reynolds numbers of tail from 300,000 to 500,000.

Figure 11.- Concluded.

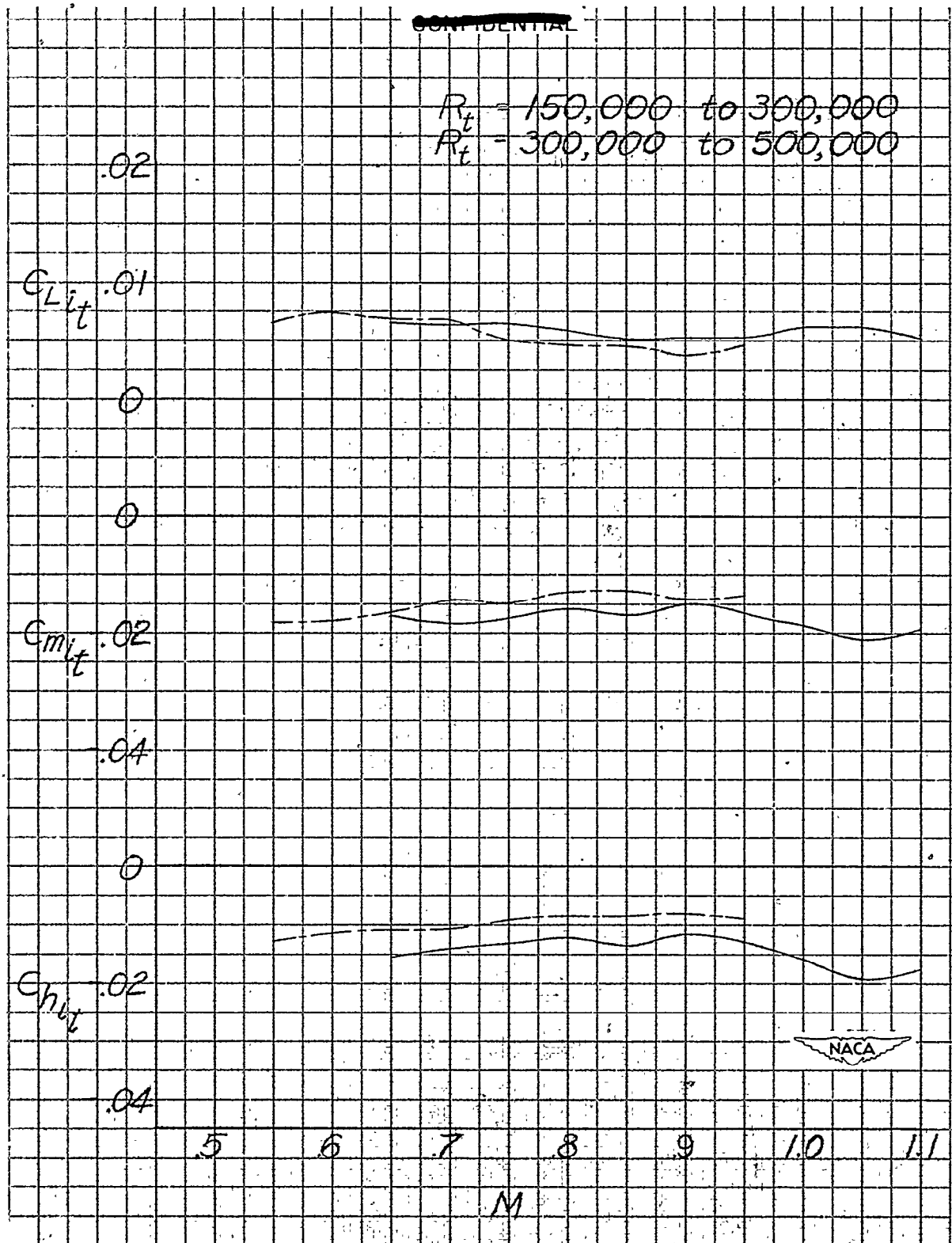


Figure 12.- Variation of $C_{L_{it}}$, $C_{m_{it}}$, and $C_{h_{it}}$ with Mach number for two Reynolds number ranges. XP-88 wing-flow model.

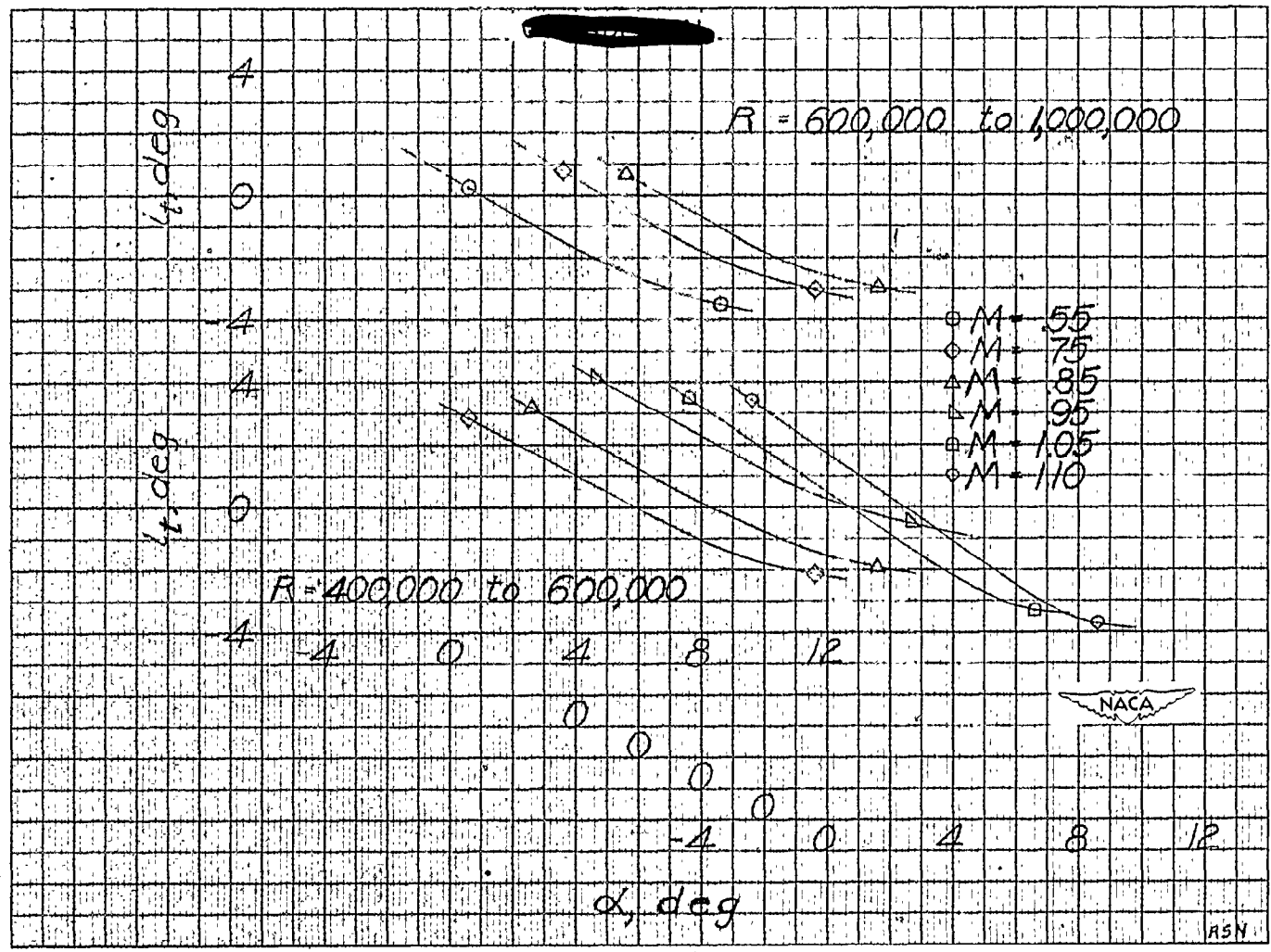


Figure 13.- Variation of tail floating angle with angle of attack at Mach numbers throughout the test range for two Reynolds number ranges. XP-88 wing-flow model with tail free.

~~CONFIDENTIAL~~

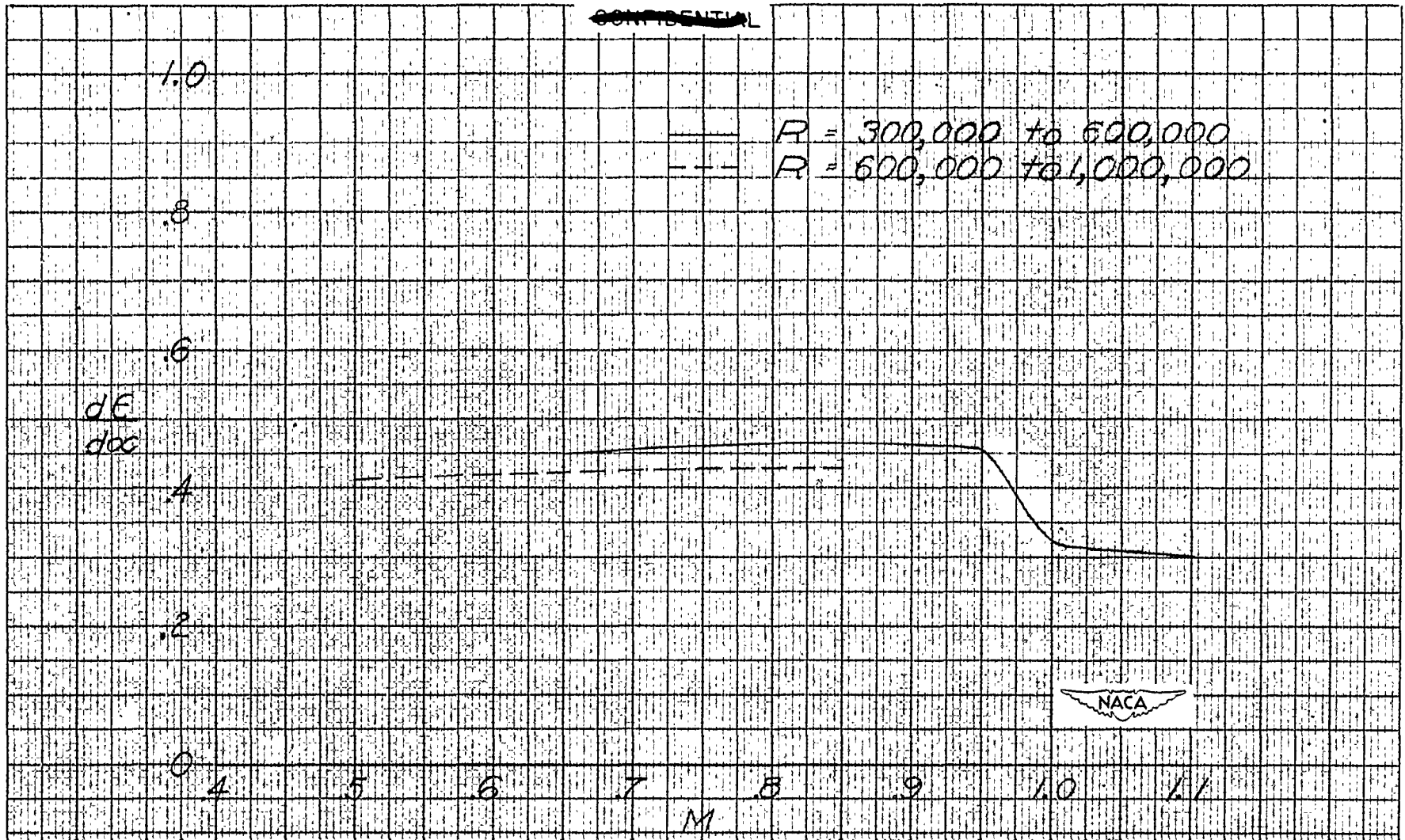


Figure 14.- Variation with Mach number of the downwash factor $d\epsilon/d\alpha$ for the flow at the tail of the XP-88 wing-flow model at small angles of attack.

~~CONFIDENTIAL~~

NASA Technical Library



3 1176 01438 5273